Carbohydrate Research, 250 (1993) 289–299
Elsevier Science Publishers B.V., Amsterdam

Chemical structure and conformational features of cell-wall polysaccharides isolated from *Aphanoascus mephitalus* and related species

Jesús Jiménez-Barbero [a], Manuel Bernabé [a], Juan Antonio Leal [b], Alicia Prieto [b] and Begoña Gómez-Miranda [b]

[a] *Grupo de Carbohidratos, Instituto de Química Orgánica, CSIC, Juan de la Cierva 3, 28006 Madrid (Spain)*
[b] *Centro de Investigaciones Biológicas, CSIC, Velázquez 144, 28006 Madrid (Spain)*

(Received March 26th, 1993; accepted May 25th, 1993)

ABSTRACT

The structures of cell-wall mannans isolated from *Aphanoascus mephitalus, A. fulvescens, A. verrucosus*, and *A. reticulisporus* have been investigated by chemical analyses and 1D and 2D ^{1}H and ^{13}C NMR techniques. It was found that all of them consists of a relatively simple comb-like structure of the disaccharide repeating block $\{\rightarrow 6)$-[α-Man*p*-$(1\rightarrow 2)$]-α-Man*p*-$(1\rightarrow\}$. The conformations around the α-$(1\rightarrow 2)$ and α-$(1\rightarrow 6)$ linkages in these kinds of polymers were also studied by using molecular mechanics and dynamics calculations, together with NOE data. The results are similar to those found within the oligosaccharide chains of glycoproteins, with a well-defined conformation for the α-$(1\rightarrow 2)$ linkage and a certain restriction around the α-$(1\rightarrow 6)$ bonding imposed by the 2-substitution.

INTRODUCTION

Mannans are constituents of many fungal cell walls, where they may play prominent physiological functions, for example, protection of the cell wall, participation in cell–cell recognition and also in the adherence of the microorganism to host cells.

In many ascomycetous yeasts[1], the antigenically relevant outer mannans have a skeleton composed of α-$(1\rightarrow 6)$-linked mannopyranosyl residues, to most of which are attached one branching moiety, each composed of chains of various lengths containing mainly α-, β(or both)-$(1\rightarrow 2)$ and/or -$(1\rightarrow 3)$ bondings (the so-called comb-like structure) as, for instance, in *Candida maltosa* and *C. tropicalis*[2].

A more complex structure (a tree-like structure) has been reported for *C. albicans*[3,4], which shows an analogous backbone of α-$(1\rightarrow 6)$-linked mannopyranosyl residues with $(1\rightarrow 2)$ and/or $(1\rightarrow 3)$ side chains, some of them, in turn, being branched.

SSDI 0008-6215(93)E0205-F

A third type of sequence has been proposed for the *C. krusei* mannan[5], which contains a main chain of mannopyranose with (1 → 2) and (1 → 6) linkages in a 3 : 1 ratio but is lightly branched, either at the 2- or 6-positions.

We now report on a highly regular and relatively simple comb-like mannan isolated from *Aphanoascus* species, which seemed also to be an appropriate structure to investigate the conformation of (1 → 2) and (1 → 6) linkages in this kind of skeleton.

MATERIALS AND METHODS

Growth of organisms, cell-wall preparation, isolation, and chemical analyses.— Four species of *Aphanoascus*, from the Dr. Guarro Collection (Facultat de Medicina, Universitat de Barcelona, 43201 Reus, Tarragona, Spain), were studied: *A. mephitalus* FMR 2113, *A. fulvescens* FMR 3392, *A. verrucosus* FMR 2141, and *A. reticulisporus* FMR 2899. Fungi culture, isolation and purification of polysaccharides from hyphae, and chemical analyses have been reported[6].

Methylation analyses.—The samples were methylated following a modification[7] of the Hakomori method[8]. Since complete methylation was not achieved, the samples were remethylated according to the procedure of Purdie and Irvine[9]. The methylated polysaccharides were hydrolysed and the resulting monosaccharides converted into partially methylated alditol acetates that were analysed as previously described[10].

NMR analysis.—NMR spectra were recorded at 70 or 40°C with a Varian XL-300 or Varian Unity 500 spectrometer. Proton chemical shifts refer to residual HDO at δ 4.36 or 4.61, respectively. Carbon chemical shifts refer to external dioxane at 67.4 ppm.

The polysaccharides (ca. 20 mg) were dissolved in D_2O (1 mL) followed by centrifugation (10 000*g*, 20 min) and further deuterium exchange. The final sample was dissolved in D_2O (0.7 mL, 99.98% D) and degassed in the NMR tube under Ar.

The parameters used for 2D experiments were as follows. The double quantum filtered DQF-COSY experiment was performed in the phase sensitive mode using the method of States et al.[11]: 256 × 1K data matrix; zero-filled to 2K × 2K; 16 scans per increment; recycle delay, 2 s; spectral width, 1500 Hz; sine-bell filtering in both dimensions. The clean 2D-TOCSY experiment[12] was carried out in the phase sensitive mode using MLEV-17 for isotropic mixing; mixing time, 150 ms; 512 × 1K data matrix; zero-filled to 2K × 2K; squared cosine-bell functions were applied in both dimensions. Similar parameters were used for the 2D rotating frame NOE[13] (ROESY, CAMELSPIN) experiment (mixing time 300 ms) and the 2D-NOESY experiment (mixing time 400 ms). The pure absorption one-bond proton–carbon correlation experiments were collected in the ^{1}H-detection mode using the HMQC pulse sequence[14] and a reverse probe; 256 × 1K data matrix; spectral widths of 8000 and 1500 Hz in F_1 and F_2; recycling delay, 1.5 s; delay

corresponding to a J value of 145 Hz; squared cosine-bell filtering in both dimensions. 16 (^{13}C-decoupled) or 32 (^{13}C-coupled) scans were accumulated per t_1 increment. The HMBC experiment[15] was performed using a delay of 60 ms and 96 scans per increment.

Molecular mechanics and dynamics calculations.—Several (ca. 30) randomly chosen starting conformations were built for a tetra- and an octa-saccharide fragment of the polysaccharide and submitted to energy minimization by using the CVFF[16] and the Discover 2.8 program[17]. *O*-Methyl groups were included at the reducing and the nonreducing ends of the fragments. Dihedral angles at the glycosidic linkages are defined as ϕ H-1′–C-1′–O-1′–C-2 and ψ C-1′–O-1′–C-2–H-2 for the α-(1 → 2) linkage, and as ϕ H-1–C-1–O-1–C-6″ and ψ C-1–O-1–C-6″–C-5″ for the α-(1 → 6) linkage. A dielectric constant of 78 D was used. The local minima found for the tetra- and octa-saccharides were then taken as starting structures for molecular dynamics (MD) calculations in vacuo at 303 K, with a dielectric constant of 78 D, and a time step of 1 fs. The equilibration time was 50 ps and the total simulation time was 550 or 1050 ps. Trajectory frames were saved every 1 ps. The trajectories were examined with the Analysis module of INSIGHT II[18].

The transient 1D-NOE experiments at 65°C were calculated according to the complete relaxation matrix method[19] by using the NOEMOL program[20] for the geometries of the main minima of the tetrasaccharide. Isotropic motion and no external relaxation was assumed in the calculation process. Since NOEs are extremely dependent on the correlation time used for the calculation, different τ_c values were tested in order to obtain the best match between the experimental and the calculated NOE for a given intraresidue proton pair. Finally, a τ_c of 1 ns was chosen. ROESY experiments were used to estimate interproton distances according to the isolated spin pair approximation (ISPA)[21].

RESULTS AND DISCUSSION

The conventional ^{1}H NMR spectra for the polysaccharides of all four species were almost identical, with the exception of that of *A. reticulisporus* which displayed small additional peaks (see Fig. 1), although the general pattern demonstrated that all of them are composed of identical skeletons. Accordingly, we carried out all the NMR experiments on the polysaccharide of *A. mephitalus*. The ^{1}H NMR spectrum showed two anomeric signals with the same relative intensity, indicating that the polysaccharide is composed of a disaccharide repeating block. The residues of the repeating unit have been labeled A and B, in order of increasing field of the H-1 resonances. The resolution of the ^{1}H NMR spectrum, combined with the DQF-COSY and TOCSY experiments (see Fig. 2a), permitted the unambiguous assignment of all resonances for both mannose residues A and B (Table I). The ^{13}C NMR resonances were assigned by comparison of the ^{1}H chemical shifts with the proton–carbon correlation data obtained from the HMQC spectrum (Fig. 2c and Table I). The relatively low-field values for C-2 and C-6 in

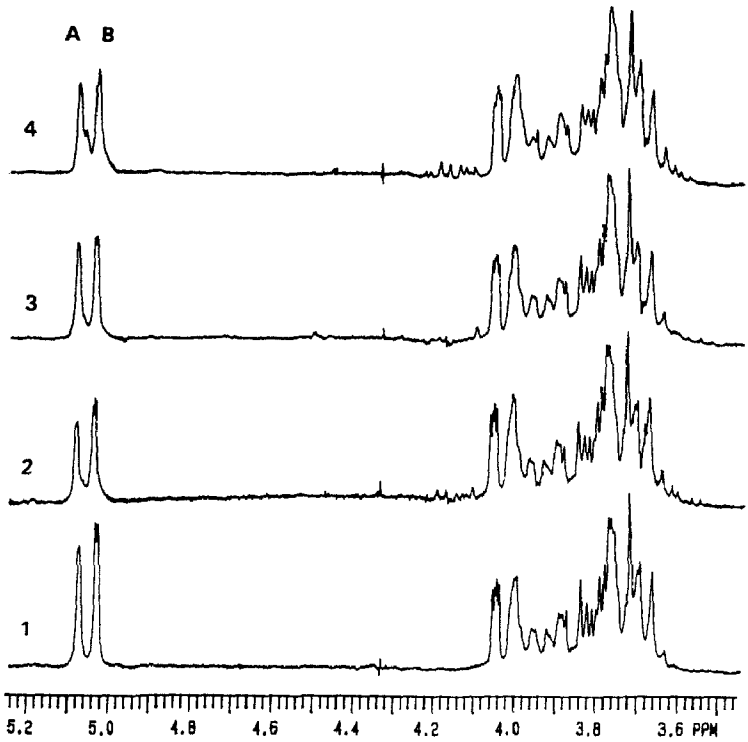

Fig. 1. ^{1}H NMR spectra (70°C, 300 MHz) of the cell-wall F1S-B mannans isolated from: 1, *Aphanoascus mephitalus*; 2, *A. fulvescens*; 3, *A. verrucosus*; and 4, *A. reticulisporus*. The anomeric protons for the units of the disaccharide repeating block have been labeled A and B.

unit A and the magnitude of the values for the carbons in unit B, as compared with published values for methyl α- and β-mannopyranosides[22], indicate a 2,6-disubstituted mannose and a terminal mannopyranose for fragments A and B, respectively, in accordance with the results from methylation analysis, which reveal a comb-like structure for the polysaccharide. To discriminate between the two possibilities of arrangement [namely a chain of Man*p*-(1 → 2)-Man*p* with mannopyranosyl substituents at position 6 in each unit, or else a Man*p*-(1 → 6)-Man*p* skeleton with mannopyranosyl substituents at position 2 in each unit], we ran a 2D-NOESY spectrum of F1S-B (Fig. 2b). In addition to expected intraresidue signals, it shows cross-peaks for H-1A/H-6A, H-1A/H-6'A, H-1A/H-5B, and H-1B/H-2A, thus supporting the second possibility. The cross-signal H-1A/H-5B indicates a slightly tilted orientation of unit B, in agreement with previous findings[23–28] (see below). A 2D-ROESY (CAMELSPIN) experiment led to analogous results. Conclusive additional evidence is provided by the long-range proton–carbon correlation HMBC experiment, which shows signals for C-1B/H-2A, C2A/H-1B, and C-6A/H-1A (Figure 3).

Concerning the configuration of the anomeric centre, a coupled HMQC experiment allowed the measurement of the values for $^1J_{C\text{-}1,H\text{-}1}$ in units A and B (174.5

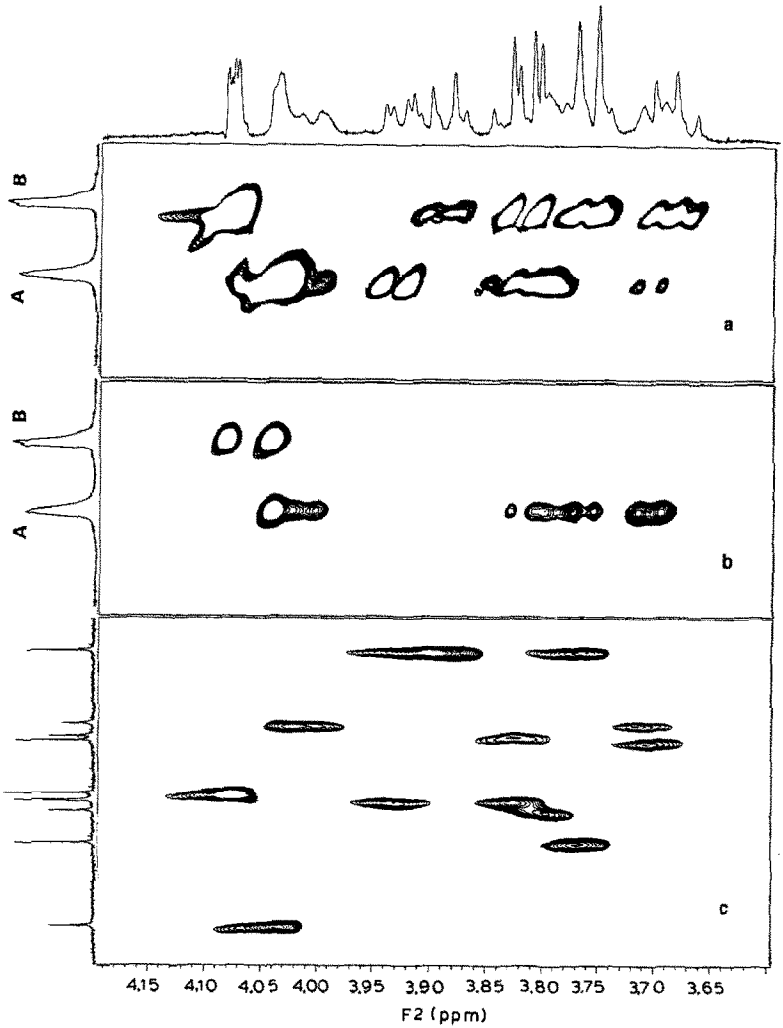

Fig. 2. 2D-NMR spectra (40°C, 500 MHz) for selected regions of the F1S-B mannan from *A. mephitalus*: a, TOCSY (HOHAHA); b, NOESY; and c, HMQC subspectra. The anomeric protons have been labeled A and B.

and 176.0 Hz, respectively) which, in accord with the low field values of chemical shifts, are in favor of the anomeric configurations being α for both residues.

Conformation around the glycosidic linkages.—The conformational analysis of the α-(1 → 2)- and α-(1 → 6)-glycosidic linkages in mannose-containing oligosaccharides has been a topic of interest during the last few years, since they are part of the carbohydrate chains of glycoproteins[23–28]. Experimental and theoretical results have shown that the α-Man-(1 → 2)-Man linkage is fairly rigid, while the α-Man-(1 → 6)-Man linkage is rather flexible, although substitution at the reducing moiety may cause an important restriction in its mobility. We decided to investi-

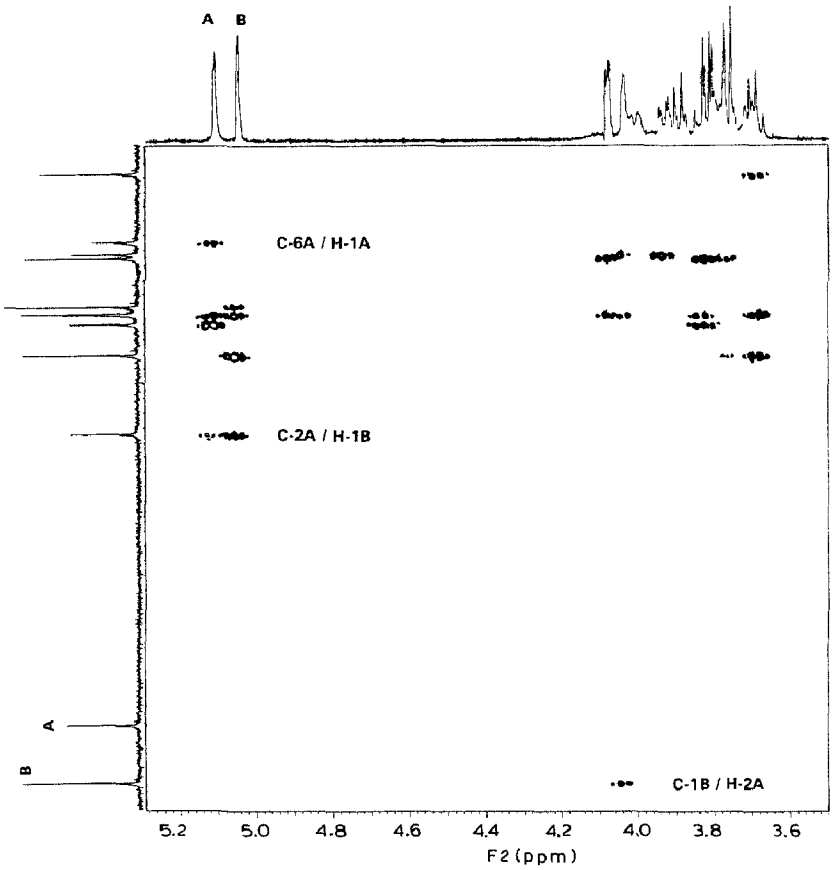

Fig. 3. 2D ^{1}H–^{13}C long-range correlation (HMBC) spectrum for the F1S-B mannan from *A. mephitalus*. Significant cross-peaks have been labeled, showing interglycosidic connections for residues A and B.

TABLE I

^{1}H and ^{13}C NMR chemical shifts (δ) and coupling constants (Hz, in brackets) for the F1S-B cell-wall polysaccharide of *A. mephitalus*

Residue	Atom signal						
	H-1	H-2	H-3	H-4	H-5	H-6	H-6′
→ 2,6)-α-Man*p*-(1 →	5.12	4.04	3.94	3.80	3.80	3.71	4.02
	(1.4)	(3.3)	(9.2)	(9.3)	(1.6)	(3.5)	
α-Man*p*-(1 →	5.06	4.08	3.82	3.69	3.77	3.77	3.90
	(1.7)	(3.3)	(9.5)	(9.5)			
	C-1	C-2	C-3	C-4	C-5	C-6	
→ 2,6)-α-Man*p*-(1 →	99.2	79.5	71.5	67.4	72.1	66.6	
α-Man*p*-(1 →	103.0	71.0	71.5	67.7	74.2	62.0	

gate the possible changes in the conformation of these linkages when they are integrated in a polymer to form a comb-like structure. On this basis, we performed molecular mechanics and dynamics calculations on tetra- and octa-saccharide models of the polysaccharide. Our results agree with previous observations for mannose-containing oligosaccharides from other laboratories[23–28]. Thus, it can be observed that, for the α-(1 → 2) linkage, there is a low energy region defined by two local minima: A, $\phi = -50°$, $\psi = -20°$; and B, $\phi = -45°$, $\psi = 35°$ (Fig. 4a); while that for the α-(1 → 6) linkage is much broader, with limits given by $\phi = -50 \pm 20°$ and $\psi = 155 \pm 65°$ (Fig. 4b). Although the CVFF is a general MD programme not specifically parametrized for oligosaccharides[29], and therefore does not include any potential for the exo-anomeric effect, its use in the conformational analysis of different oligosaccharides has produced satisfactory results[30]. The different low-energy conformations were used as input geometries for different 550- and 1050-ps MD simulations at 303 K. The trajectories of several simulations are displayed in Fig. 4. No chair-to-chair or chair-to-boat interconversions were observed. The average ϕ and ψ angles were $-42°$ and -18 or 35°, and 70° and from 160 to $-160°$, for the α-(1 → 2) and the α-(1 → 6) linkage, respectively, depending on the starting conformation. After the corresponding equilibration periods (ca. 50 ps), it can be observed that the simulations remained in the low energy regions (Figs. 4c and d).

NMR spectroscopy can be used either qualitatively or quantitatively to verify the presence of these conformers[31]. All the low energy region for the α-(1 → 2) linkage shows short distances between H-2 and H-1′, and H-1 and H-5′. On the other hand, the low energy region for the α-(1 → 6) linkage is defined by interresidue contacts between H-1′ and H-$6_{pro\text{-}R}$ or H-$6_{pro\text{-}S}$ depending on ϕ, ψ, and ω torsion angles. These structural characteristics are gathered in Table II. The observation of one or two interresidue NOEs imposes constraints in the conformational map, showing the presence of a given conformer[32]. The analysis of vicinal $^3J_{H,H}$ coupling constants indicated that the pyranoid rings are in the expected $^4C_1$ chair conformation. In addition, $J_{5,6}$ and $J_{5,6'}$ for the α-(1 → 6) linkage (2.0 and 3.5 Hz, respectively) allowed us to estimate an important population of the *gg* rotamer around the C-5–C-6 bond[27,33]. Thus, the coupling constants around this linkage agree with a 70 : 30 distribution of *gg* : *gt* rotamers.

Analysis of NOE data.—Qualitatively, the presence of strong NOE between H-1′ and H-2, and between H-5′ and H-1 implies that the α-(1 → 2) linkage spends most of its time in the low energy region defined by local minima A and B. The differentiation among these minima is more difficult since their expected interresidue contacts are very similar. An estimation of interresidue distances may be obtained by use of the isolated spin pair approximation (ISPA), using the volumes of the cross-peaks between proton pairs in NOESY or ROESY spectra acquired with a relatively short mixing time (Table III). This approximation leads to H-1′–H-2 distances in the range 2.1–2.5 Å and H-5′–H-1 distances in the range 2.3–2.7 Å as expected for the low energy region, in agreement with both A and B

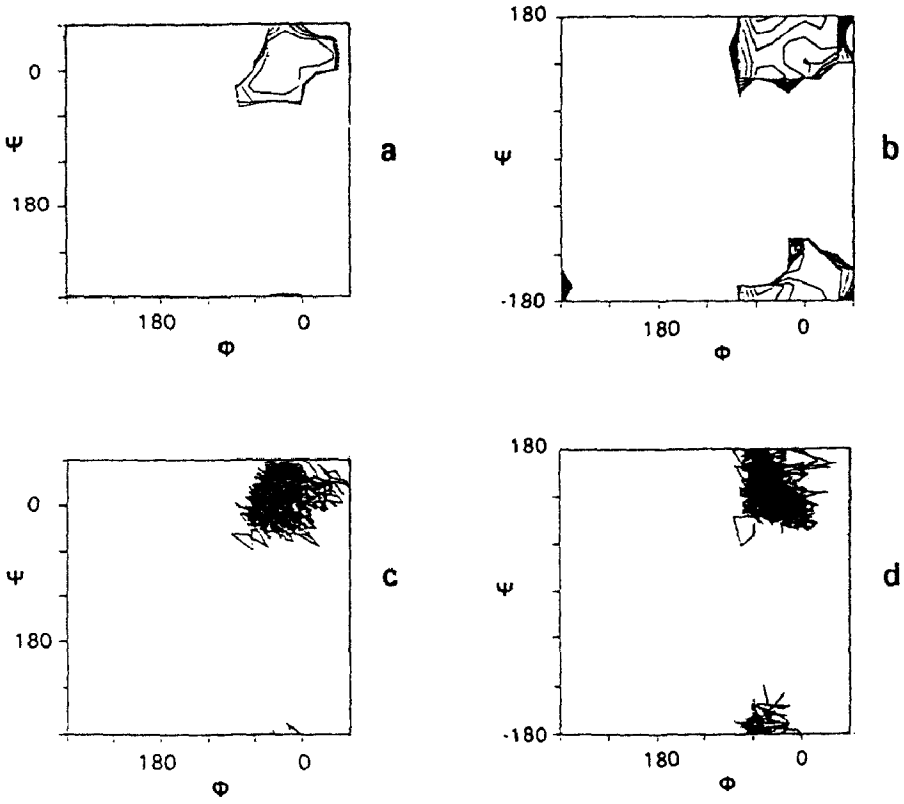

Fig. 4. Ramachandran-type plot of the isoenergy contours of a, α-(1 → 2); and b, α-(1 → 6) linkages; according to the DICOVER-CVFF program. Trajectory of c, one of the α-(1 → 2); and d, one of the α-(1 → 6) linkages during 1-ns MD simulations at 303 K.

conformers. The corresponding average distances from MD simulations are 2.3 and 2.5 Å, respectively. Nevertheless, a more rigorous approach for evaluation of the experimental data is to use the geometries of the different conformers to

TABLE II

Relevant interatomic distances (Å) for the low energy conformers of the polysaccharide F1S-B

H–H	Conformer (ϕ / ψ)			
	A(−50, −20)	B(−40, −35)	C(−58, −160)	D(−54, −170)
	Glycosidic linkage			
	α-(1 → 2)	α-(1 → 2)	α-(1 → 6) *gt*	α-(1 → 6) *gg*
H-1′–H-2	2.53	2.28		
H-1′–H-2′	2.45	2.45		
H-1–H-5′	2.66	2.63		
H-1–H-6″$_R$			2.85	3.14
H-1–H-6″$_S$			2.70	2.42
H-1–H-5″			4.48	4.71

TABLE III

Experimental NOESY and ROESY intensities (mixing time, 0.3 s) for compound F1S-B at 65°C in D_2O solution

	Cross-peak intensity (%)					
	H-1′/2	H-1′/2	H-1/2	H-1/5′	H-1/6″a	H-1/6″b
NOESY	8	9	8	6	5	2
ROESY	8	7	7	5	4	2

calculate the expected NOEs via a complete relaxation matrix approach[34], using either a single conformational model or an average[35] according to a Boltzmann distribution function at a given temperature[36]. The observed results are collected in Table IV. A satisfactory match between the calculated and experimental intensities of H-1–H-2 and H-1′–H-2′ in transient and steady-state NOE measurements was obtained by using average correlation times of 1 ns. The comparison among the observed and calculated interresidue cross-peaks H-1′–H-2 and H-5′–H-1 for the different individual conformers indicated that the best match was found by considering local minimum A for the α-(1 → 2) linkage, although the presence of a certain motion around the glycosidic bond cannot be neglected. With regard to the α-(1 → 6) linkage, the results are indicative of higher flexibility, since none of the individual conformers could match all the NOE values at the same time. Nevertheless, the observed NOEs and coupling constants are closer to the results expected for an important contribution of the *gg* rotamer and a ψ value of ca. −160°. Fig. 5 shows a stereoscopic view of the global minimum of the octasaccharide fragment used in the calculations, while in Fig. 6 the α-(1 → 2)-linked mannoses have been hidden to show the main chain conformation.

In conclusion, according to our results, the conformations around the glycosidic bonds of the polysaccharide F1S-B of *A. mephitalus* are similar to those observed for the α-(1 → 2) linkage within the oligosaccharide chains of glycoproteins[13–18],

TABLE IV

Experimental and calculated 1D-NOEs (irradiation time, 0.700 s) for the polysaccharide F1S-B at 65°C in D_2O solution upon saturation of H-1′ or H-1 signals

	Observed NOE for signal (%)					
	H-2 [a]	H-2′ [a]	H-5′ [b]	H-2 [b]	H-$6''_R$ [b]	H-$6''_S$ [b]
	8	8	9	7	6	5
	Calculated NOE (%) for the tetrasaccharide model [c]					
	H-2 [a]	H-2′ [a]	H-5′ [b]	H-2 [b]	H-6a″ [b]	H-6b″ [b]
Conf. A	7	8	9	7		
Conf. B	14	8	5	8		
Conf. C					5	5
Conf. D					7	3

[a] Irradiating H-1′. [b] Irradiating H-1, [c] Using the full-matrix relaxation method and $\tau_c = 1.0 \times 10^{-9}$s.

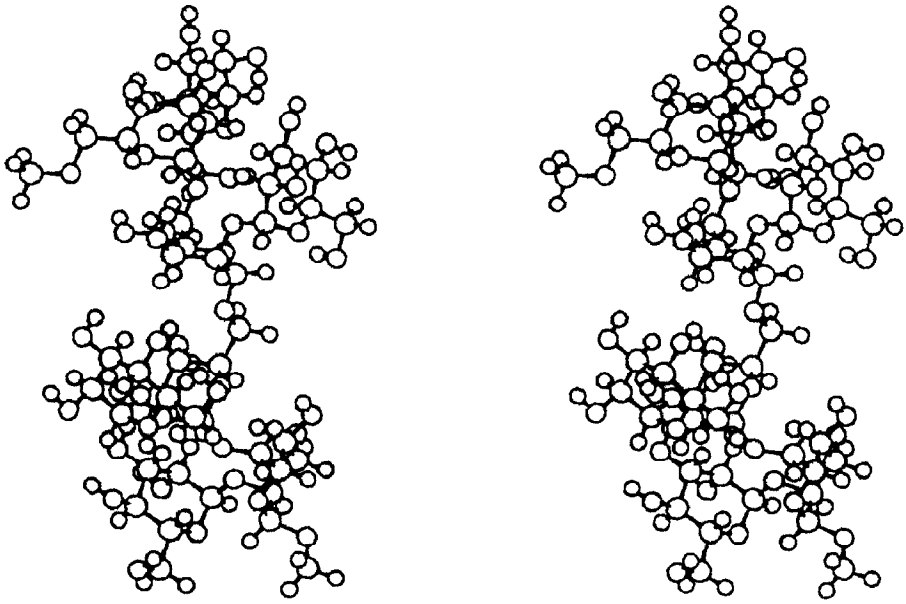

Fig. 5. Stereoscopic view of the global minimum conformation of the model octasaccharide used in the MM and MD calculations.

Fig. 6. Stereoscopic view of the global minimum conformation of the model octasaccharide used in the MM and MD calculations. The α-(1 → 2)-linked mannopyranosides have been omitted to show the main chain conformation.

with a well-defined conformation around the the α-(1 → 2) linkage and a certain restriction imposed by the substitution at both mannopyranosyl residues around the α-(1 → 6) linkage, as observed in triantennary or similar oligosaccharides.

ACKNOWLEDGMENTS

This work was supported by Grants PB 87/0243 and PB 91/0054 from Dirección General de Investigación Científica y Técnica.

REFERENCES

1 P.A.J. Gorin and J.F.T. Spencer, *Adv. Appl. Microbiol.*, 13 (1970) 25–89.
2 E.V. Bovina, V.V. Deryabin, V.N. Gagloev, and N.G. Serebryakov, *Prikl. Biokhim. Mikrobiol.*, 24 (1988) 218–225.

3 M. Suzuki and Y. Fukazawa, *Microbiol. Immunol.*, 26 (1982) 387–402.
4 G. Kogan, V. Pavliak, and L. Masler, *Carbohydr. Res.*, 172 (1988) 243–253.
5 G. Kogan, V. Pavliak, J. Sandula, and L. Masler, *Carbohydr. Res.*, 184 (1988) 171–182.
6 J.A. Leal, B. Gómez-Miranda, M. Bernabé, J. Cano, and J. Guarro, *Mycol. Res.*, 96 (1992) 363–368.
7 P.-E. Jansson, L. Kenne, H. Liedren, B. Lindberg, and J. Lönngren, *Chem. Commun. Univ. Stockholm*, 8 (1976).
8 S. Hakomori, *J. Biochem. (Tokyo)*, 55 (1964) 205–208.
9 T. Purdie and J.C. Irvine, *J. Chem. Soc.*, 83 (1903) 1021.
10 B. Gómez-Miranda, A. Prieto, and J.A. Leal, *FEMS Microbiol. Lett.*, 70 (1990) 331–336.
11 D.J. States, R.A. Haberkorn, and D.J. Ruben, *J. Magn. Reson.*, 48 (1982) 286–292.
12 C. Griesinger, G. Otting, K. Wüthrich, and R.R. Ernst, *J. Am. Chem. Soc.*, 110 (1988) 7870–7872.
13 A.A. Bothner-By, R.L. Stephens, J.-M. Lee, C.D. Warren, and R.W. Jeanloz, *J. Am. Chem. Soc.*, 106 (1984) 811–813; A. Bax and D.G. Davis, *J. Magn. Reson.*, 63 (1985) 207–213.
14 A. Bax and S. Subramanian, *J. Magn. Reson.*, 67 (1986) 565–569.
15 A. Bax and M.F. Summers, *J. Am. Chem. Soc.*, 108 (1986) 565–569.
16 A.T. Hagler, S. Lifson, and P. Dauber, *J. Am. Chem. Soc.*, 101 (1979) 5122–5130.
17 Discover 2.8 Program, Biosym Technologies Inc., San Diego, CA.
18 Insight 2.1.0 Program, Biosym Technologies Inc., San Diego, CA.
19 T. Peters, J.R. Brisson, and D.R. Bundle, *Can. J. Chem.*, 68 (1990) 979–988, and references therein.
20 M. Forster, C. Jones, and B. Mulloy, *J. Mol. Graph*, 7 (1989) 196–201; M.J. Forster, *J. Comput. Chem.*, 12 (1991) 292–300.
21 D. Neuhaus and M.P. Williamson, *The Nuclear Overhauser Effect in Structural and Conformational Analysis*, VCH, New York, 1989.
22 K. Bock, C. Pedersen, and H. Pedersen, *Adv. Carbohydr. Chem. Biochem.*, 42 (1984) 193–225.
23 H. Paulsen, T. Peters, V. Sinnwell, M. Heume, and B. Meyer, *Carbohydr. Res.*, 156 (1986) 87–106; H. Paulsen, T. Peters, V. Sinnwell, and B. Meyer, *ibid.*, 165 (1987) 251–266.
24 D.A. Cumming and J.P. Carver, *Biochemistry*, 26 (1987) 6664–6676, 6676–6683.
25 S.W. Homans, A. Pastore, R.A. Dwek, and T.W. Rademacher, *Biochemistry*, 26 (1987) 6649–6655; C.J. Edge, U.C. Singh, R. Bazzo, G.L. Taylor, R.A. Dwek, and T.W. Rademacher, *ibid.*, 29 (1990) 1971–1974.
26 T. Peters, *Liebigs Ann. Chem.*, (1991) 135–144; A. Helander, L. Kenne, S. Oscarson, T. Peters, and J.R. Brisson, *Carbohydr. Res.*, 230 (1992) 299–318; T. Peters, B. Meyer, R. Stuike-Prill, R. Somorjai, and J.R. Brisson, *ibid.*, 238 (1993) 49–74.
27 H. Hori, Y. Nishida, H. Ohrui, H. Meguro, and J. Ozawa, *Tetrahedron Lett.*, 29 (1988) 4457–4460.
28 P. de Waard, B.R. Leeflang, J.F.G. Vliegenthart, R. Boelens, G.W. Vuister, and R. Kaptein, *J. Biomol. NMR*, 2 (1992) 211–226.
29 S.W. Homans, *Biochemistry*, 29 (1990) 9110–9118; S.W. Homans and M. Forster, *Glycobiology*, 2 (1992) 143–151.
30 H.C. Siebert, G. Reuter, R. Schauer, C.W. von der Lieth, and J. Dabrowski, *Biochemistry*, 31 (1992) 6962–6971; A.E. Aulabaugh, R.C. Crouch, G.E. Martin, A. Ragouzeos, J.P. Shockcor, T.D. Spitzer, R.D. Farrant, B.D. Hudson, and J.C. Lindon, *Carbohydr. Res.*, 230 (1992) 201–212.
31 K. Bock, *Pure Appl. Chem.*, 55 (1983) 605–622.
32 B. Meyer, *Top. Curr. Chem.*, 154 (1990) 141–208.
33 Y. Nishida, H. Ohrui, and H. Meguro, *Tetrahedron Lett.*, 25 (1984) 1575–1578; Y. Nishida, H. Hori, H. Ohrui, and H. Meguro, *J. Carbohydr. Chem.*, 7 (1988) 239–250.
34 J.R. Brisson, and J.P. Carver, *Biochemistry*, 22 (1983) 1362–1368.
35 K. Bock, H. Lönn, and T. Peters, *Carbohydr. Res.*, 198 (1990) 375–380.
36 A. Imberty, V. Tran, and S. Perez, *J. Comput. Chem.*, 11 (1989) 205–216.